molecules

MDPI

Article

Phenylethanoid and Phenylmethanoid Glycosides from the Leaves of *Ligustrum robustum* and Their Bioactivities

Shi-Hui Lu [1,*,†], Hao-Jiang Zuo [2,†], Jing Huang [3,*], Ran Chen [4], Jia-Ping Pan [1] and Xiu-Xia Li [5,*]

[1] College of Pharmacy, Youjiang Medical University for Nationalities, Baise 533000, China
[2] Department of Laboratory Science of Public Health, West China School of Public Health, Sichuan University, Chengdu 610041, China
[3] Key Laboratory of Drug Targeting, Ministry of Education, West China School of Pharmacy, Sichuan University, Chengdu 610041, China
[4] Institute of Life Science, Youjiang Medical University for Nationalities, Baise 533000, China
[5] Nursing School, Youjiang Medical University for Nationalities, Baise 533000, China
* Correspondence: lushihui0818@126.com (S.-H.L.); huangj_pharm@scu.edu.cn (J.H.); axia-883333@163.com (X.-X.L.)
† These authors contributed equally to this work.

Abstract: The phytochemical study on the leaves of *Ligustrum robustum*, which have been used as Ku-Ding-Cha, led to the isolation and identification of three new phenylethanoid glycosides and three new phenylmethanoid glycosides, named ligurobustosides R_1 (**1b**), R_{2-3} (**2**), R_4 (**3**), S_1 (**4b**), S_2 (**5**), and S_3 (**6**), and five reported phenylethanoid glycosides (**7**–**11**). In the bioactivity test, (*Z*)-osmanthuside B_6 (**11**) displayed strong fatty acid synthase (FAS) inhibitory activity (IC_{50}: 4.55 ± 0.35 μM) as the positive control orlistat (IC_{50}: 4.46 ± 0.13 μM), while ligurobustosides R_4 (**3**) and S_2 (**5**), ligupurpuroside B (**7**), *cis*-ligupurpuroside B (**8**), ligurobustoside N (**9**), osmanthuside D (**10**), and (*Z*)-osmanthuside B_6 (**11**) showed stronger ABTS radical scavenging activity (IC_{50}: 2.68 ± 0.05~4.86 ± 0.06 μM) than the positive control L-(+)-ascorbic acid (IC_{50}: 10.06 ± 0.19 μM). This research provided a theoretical basis for the leaves of *L. robustum* as a tea with function in treating obesity and diabetes.

Keywords: *Ligustrum robustum*; phenylethanoid glycoside; phenylmethanoid glycosides; FAS; α-glucosidase; antioxidant; anti-obesity; hypoglycemic

Citation: Lu, S.-H.; Zuo, H.-J.; Huang, J.; Chen, R.; Pan, J.-P.; Li, X.-X. Phenylethanoid and Phenylmethanoid Glycosides from the Leaves of *Ligustrum robustum* and Their Bioactivities. *Molecules* **2022**, *27*, 7390. https://doi.org/10.3390/molecules27217390

Academic Editor: Thomas J. Schmidt

Received: 19 September 2022
Accepted: 28 October 2022
Published: 31 October 2022

1. Introduction

Ku-Ding-Cha, a tea with functions in clearing heat, removing toxins, and treating obesity and diabetes, has been applied widely in Southwest China for nearly 2000 years [1,2]. It was derived from the leaves of more than 30 plants belonging to 13 genera in 12 families [3]. *Ligustrum robustum* (Roxb.) Blume (Oleaceae), classified as a food by the Chinese Ministry of Health since 2011, has been used as Ku-Ding-Cha in Southwest China [4,5]. In the previous investigations on *L. robustum* [1–16], more than 60 chemical constituents, including monoterpenoid glycosides, phenylethanoid glycosides, phenylmethanoid glycosides, iridoid glycosides, flavonoid glycosides, lignan glycosides, and triterpenoids, were discovered, and the antioxidative, anti-obesity, and anti-inflammatory effects of the aqueous extract, the inhibitory activities on FAS, α-glucosidase, and α-amylase, and the antioxidant effects of some constituents, were observed. To further elucidate the active components for preventing obesity and diabetes, the phytochemical and biological study on the leaves of *L. robustum*, which had been performed preliminarily [12,13], was carried out. As a result, three new phenylethanoid glycosides and three new phenylmethanoid glycosides, named ligurobustosides R_1 (**1b**), R_{2-3} (**2**), R_4 (**3**), S_1 (**4b**), S_2 (**5**), and S_3 (**6**), and five reported phenylethanoid glycosides (**7**–**11**) (Figure 1) were isolated from the leaves of *L. robustum*. This article discusses the isolation and structure identification of compounds

1–11 and deals with their inhibitory effects on FAS, α-glucosidase, α-amylase, and their antioxidant activities.

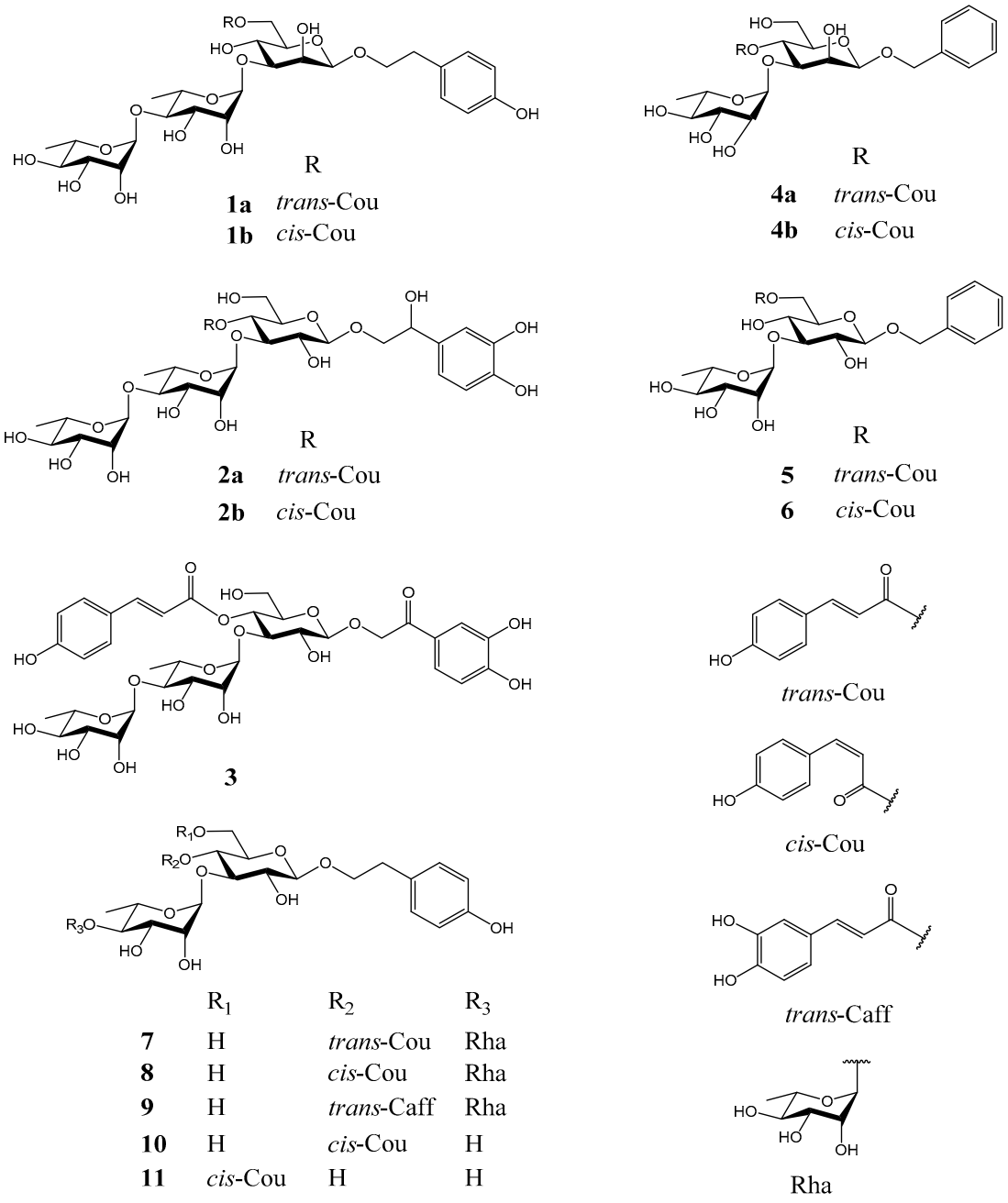

Figure 1. Structures of compounds **1–11** from the leaves of *L. robustum*.

2. Material and Methods

2.1. General Experimental Procedure

Optical rotation value was determined with an AUTOPOL VI automatic polarimeter (Rudolph, Hackettstown, NJ, USA). The UV spectrum was measured on a UV2700 spectrophotometer (Shimadzu, Kyoto, Japan). IR absorption spectrum was carried out with a PerkinElmer Spectrum Two FT-IR spectrometer (PerkinElmer, Waltham, MA, USA). NMR spectra were recorded using an Agilent 600/54 Premium Compact NMR spectrometer (Agilent, Santa Clara, CA, USA) (^{1}H at 600 MHz, ^{13}C at 150 MHz) or a Bruker Ascend^{TM} 400 NMR spectrometer (Bruker, Germany) (^{1}H at 400 MHz, ^{13}C at 100 MHz) with CD_3OD (compound **3**: CD_3OD + DMSO-d_6) as the solvent at 25 °C. Chemical shifts are reported in

δ (ppm) with tetramethylsilane (TMS) as the internal standard, while coupling constants (*J*) are expressed in Hz. High-resolution electrospray ionization mass spectroscopy (HRESIMS) was measured on a Waters Q-TOF Premier mass spectrometer (Waters, Milford, MA, USA).

Column chromatography (CC) was carried out on silica gel (SiO_2: 200–300 mesh, Qingdao Ocean Chemical Industry Co., Pingdu, Qingdao, China), polyamide (60–90 mesh, Jiangsu Changfeng Chemical Industry Co., Gulou, Nanjing, China), and MCI-gel CHP-20P (75–150 μm, Mitsubishi Chemical Co., Tokyo, Japan). Preparative HPLC was carried out on a GL3000-300 mL system instrument (Chengdu Gelai Precision Instruments Co., Ltd., Dayi, Chengdu, China) with a UV-3292 detector (detection wavelength 215 nm) and a GL C-18 column (particle size 5 μm, 50 × 450 mm), eluting with MeOH-H_2O at 30 mL/min. TLC was performed on precoated HPTLC Fertigplatten Kieselgel 60 F_{254} plates (Merck, Rahway, NJ, USA), and the spots were visualized by spraying with 10% sulfuric acid ethanolic solution or α-naphthol-sulfuric acid solution and baking at 105 °C for 2–5 min. UV-vis absorbance was determined on a Spark 10M microplate reader (Tecan Trading Co. Ltd., Shanghai, China) or a UV2700 spectrophotometer (Shimadzu, Kyoto, Japan). Acetyl-coenzyme A (Ac-CoA) and NADPH were purchased from Zeye Biochemical Co., Ltd. (Shanghai, China). Methylmalonyl coenzyme A tetralithium salt hydrate (Mal-CoA) was obtained from Sigma-Aldrich (St. Louis, MO, USA). 2,2-Diphenyl-1-picrylhydrazyl (DPPH) was purchased from Macklin Biochemical Co., Ltd. (Shanghai, China). 2,2′-Azino-bis(3-ethylbenzthiazoline-6-sulphonic acid) ammonium salt (ABTS) was obtained from Aladdin Industrial Co., Ltd. (Shanghai, China).

2.2. Plant Material

The leaves of *L. robustum* were harvested in April 2017 from Yibin City, Sichuan Province, China, and authenticated by Professor Guo-Min Liu (Kudingcha Research Institute, Hainan University, China). A voucher specimen (No. 201704lsh) was conserved at West China School of Pharmacy, Sichuan University, China.

2.3. Extraction and Isolation

The fresh leaves of *L. robustum* were agitated and baked at 120 °C for 50 min and then smashed. The raw powder (7.0 kg) was extracted with 70% ethanol (28 L × 1) under reflux in a multi-function extractor for 2 h [13]. The ethanol extract was percolated and condensed in vacuo to gain a paste (2.2 kg). The paste was dissolved in 3 L 95% ethanol, and then 3 L purified water was infunded to sediment the chlorophyll. After percolation, the filtrate was condensed in vacuo to obtain a residue (1.0 kg). The residue was separated on a silica gel column, eluting with CH_2Cl_2-MeOH (10:0–0:10), to yield Fr. I (84 g), Fr. II (145 g), Fr. III (93 g), and Fr. IV (70 g). Fr. II was isolated repeatedly by CC on silica gel, eluting with CH_2Cl_2-MeOH-H_2O (200:10:1–80:20:2) or EtOAc-MeOH-H_2O (100:4:2–100:6:2), and then separated on polyamide column (EtOH-H_2O, 1:9–6:4) and MCI column (MeOH-H_2O, 3:7–8:2), and purified finally by preparative HPLC (MeOH-H_2O, 40:60–65:35) and silica gel column (EtOAc-MeOH-H_2O, 100:4:2–100:6:2), or recrystallized in 70% methanol, to afford **1** (107.4 mg), **4** (11.2 mg), **5** (3.5 mg), **6** (8.3 mg), **7** (14.4 mg), **8** (15.8 mg), **10** (21.3 mg), and **11** (139.4 mg). Fr. III was separated twice by CC on silica gel (EtOAc-MeOH-H_2O, 100:4:2–100:20:10) and then subjected to polyamide column (EtOH-H_2O, 0:10–6:4) and MCI column (MeOH-H_2O, 3:7–5:5), and purified at last by preparative HPLC (MeOH-H_2O, 30:70–50:50) and silica gel column (EtOAc-MeOH-H_2O, 100:10:5), to give **2** (37.3 mg), **3** (22.4 mg), and **9** (13.5 mg).

Compound **1**: white amorphous powder. $[\alpha]^{20}_D$ −43.9 (c 0.28, MeOH); UV (MeOH) λ_{max}: (log ε) 212 (4.1), 227 (4.2), 317 (4.4) nm; IR (film) ν_{max}: 3368, 2930, 1690, 1604, 1515, 1445, 1261, 1039, 981, 829 cm^{-1}; ^1H NMR (CD_3OD, 400 MHz) data, see Table 1; ^{13}C NMR (CD_3OD, 100 MHz) data, see Table 2; HRESIMS *m*/*z* 761.2634 $[M + Na]^+$ (calculated for $C_{35}H_{46}NaO_{17}$, 761.2633).

Table 1. ^{1}H NMR (400 MHz) data of compounds **1–3** from *L. robustum* [a].

No	1b [b]	2a [b]	2b [b]	3 [c]
2	7.01 d (8.0)	6.72 d (2.0)	6.72 d (2.0)	7.46 br. s
3	6.67 d (8.0)			
5	6.67 d (8.0)	6.74 d (8.0)	6.74 d (8.0)	6.89 d (8.4)
6	7.01 d (8.0)	6.83 dd (8.0, 2.0)	6.83 dd (8.0, 2.0)	7.47 br. d (8.4)
7	2.83 t (7.2)	4.75 dd (9.6, 3.2)	4.75 dd (9.6, 3.2)	
8	3.72 m	3.56–3.72 m	3.56–3.72 m	4.98 d (16.8)
	3.96 m	3.90–3.98 m	3.90–3.98 m	5.26 d (16.8)
Glc or Man				
1′	4.28 d (7.6)	4.41 d (8.0)	4.43 d (8.0)	4.54 d (7.6)
2′	3.31 m	3.46 m	3.45 m	3.52 m
3′	3.54 m	3.83 m	3.80 m	3.87 m
4′	3.38 m	4.95 t (9.6)	4.90 t (9.6)	4.96 t (9.6)
5′	3.53 m	3.56 m	3.51 m	3.61 m
6′	4.29 dd (11.6, 6.4)	3.53 m	3.53 m	3.54 m
	4.46 dd (11.6, 2.0)	3.61 m	3.61 m	3.61 m
Inner-Rha				
1″	5.17 d (2.0)	5.22 d (2.0)	5.21 d (2.0)	5.22 br. s
2″	3.89 m	3.88 dd (3.2, 2.0)	3.82 dd (3.2, 2.0)	3.87 m
3″	3.84 dd (9.6, 3.2)	3.68 dd (9.2, 3.2)	3.68 dd (9.2, 3.2)	3.66 m
4″	3.53 m	3.40 m	3.40 m	3.40 m
5″	4.10 m	3.60 m	3.60 m	3.60 m
6″	1.28 d (6.0)	1.09 d (6.0)	1.08 d (6.0)	1.10 d (6.0)
Outer-Rha				
1‴	5.19 d (1.6)	5.04 d (2.0)	5.06 d (2.0)	5.06 br. s
2‴	3.94 m	3.90 dd (3.2, 2.0)	3.90 dd (3.2, 2.0)	3.88 m
3‴	3.60 dd (9.6, 3.2)	3.51 m	3.51 m	3.49 m
4‴	3.39 m	3.32 m	3.32 m	3.32 m
5‴	3.70 m	3.46 m	3.46 m	3.46 m
6‴	1.25 d (6.4)	1.04 d (6.0)	1.04 d (6.0)	1.06 d (6.0)
Cou				
2⁗	7.62 d (8.4)	7.49 d (8.8)	7.72 d (8.8)	7.54 d (8.4)
3⁗	6.75 d (8.4)	6.82 d (8.8)	6.77 d (8.8)	6.87 d (8.4)
5⁗	6.75 d (8.4)	6.82 d (8.8)	6.77 d (8.8)	6.87 d (8.4)
6⁗	7.62 d (8.4)	7.49 d (8.8)	7.72 d (8.8)	7.54 d (8.4)
7⁗	6.86 d (12.8)	7.67 d (16.0)	6.99 d (12.8)	7.68 d (16.0)
8⁗	5.79 d (12.8)	6.33 d (16.0)	5.76 d (12.8)	6.37 d (16.0)

[a] Coupling constants (*J* values in Hz) are shown in parentheses. [b] In CD_3OD. [c] In CD_3OD + DMSO-d_6.

Table 2. ^{13}C NMR data of compounds **1–3** from *L. robustum*.

No	1b [a]	2a [b]	2b [b]	3 [c]
1	130.6	133.6	133.6	127.9
2	130.9	119.0	119.0	115.8
3	116.1	146.3	146.3	146.7
4	156.7	146.1	146.1	152.9
5	116.1	116.2	116.2	117.0
6	130.9	114.6	114.6	122.9
7	36.4	74.2	74.2	196.4
8	72.3	76.7	76.7	72.2
Glc or Man				
1′	104.2	104.6	104.4	103.9
2′	75.7	76.4	76.4	76.2
3′	83.6	81.2	81.1	81.1
4′	70.4	70.3	70.1	70.4
5′	75.2	76.1	75.9	76.2
6′	64.4	62.2	62.3	62.2
Inner-Rha				
1″	103.2	102.6	102.7	102.6
2″	72.8	72.8	72.8	72.7
3″	73.0	72.6	72.6	72.6
4″	81.1	81.6	81.5	81.2
5″	68.4	68.9	68.6	68.8
6″	18.6	19.1	18.9	19.4

Table 2. *Cont.*

No	1b [a]	2a [b]	2b [b]	3 [c]
Outer-Rha				
1‴	102.4	103.5	103.4	103.3
2‴	72.3	72.3	72.2	72.3
3‴	72.3	72.3	72.2	72.3
4‴	73.8	73.8	73.9	73.6
5‴	70.4	70.3	70.1	70.3
6‴	17.8	17.7	17.8	18.1
Cou				
1⁗	127.5	126.9	127.5	126.9
2⁗	133.7	131.5	134.3	131.5
3⁗	115.9	117.1	115.0	117.2
4⁗	160.1	161.5	160.3	161.4
5⁗	115.9	117.1	115.0	117.2
6⁗	133.7	131.5	134.3	131.5
7⁗	145.3	147.6	147.5	147.3
8⁗	116.3	114.7	115.7	114.9
CO	168.1	168.1	166.8	167.6

[a] At 100 MHz, in CD_3OD. [b] At 150 MHz, in CD_3OD. [c] At 100 MHz, in CD_3OD + DMSO-d_6.

Compound **2**: white amorphous powder. $[\alpha]^{23}_{D}$ −62.1 (*c* 0.49, MeOH); UV (MeOH) λ_{max} (log ε): 213 (4.1), 226 (4.2), 318 (4.4) nm; IR (film) ν_{max}: 3356, 2931, 1693, 1630, 1603, 1515, 1448, 1263, 1040, 982, 834, 803 cm^{-1}; ^1H NMR (CD_3OD, 400 MHz) data, see Table 1; ^{13}C NMR (CD_3OD, 150 MHz) data, see Table 2; HRESIMS *m*/*z* 793.2536 $[M + Na]^+$ (calculated for $C_{35}H_{46}NaO_{19}$, 793.2531).

Compound **3**: yellow amorphous powder. $[\alpha]^{23}_{D}$ −46.0 (*c* 0.45, MeOH); UV (MeOH) λ_{max} (log ε): 213 (4.1), 227 (4.2), 316 (4.4) nm; IR (film) ν_{max}: 3402, 1652, 1604, 1048, 1029, 823, 761 cm^{-1}; ^1H NMR (CD_3OD + DMSO-d_6, 400 MHz) data, see Table 1; ^{13}C NMR (CD_3OD + DMSO-d_6, 100 MHz) data, see Table 2; HRESIMS *m*/*z* 791.2371 $[M + Na]^+$ (calculated for $C_{35}H_{44}NaO_{19}$, 791.2374).

Compound **4**: white amorphous powder. $[\alpha]^{20}_{D}$ −122.4 (*c* 0.25, MeOH); UV (MeOH) λ_{max} (log ε): 210 (3.9), 230 (3.9), 315 (4.4) nm; IR (film) ν_{max}: 3360, 2929, 1695, 1603, 1449, 1330, 1259, 1157, 1021, 912, 833, 741, 699 cm^{-1}; ^1H NMR (CD_3OD, 400 MHz) data, see Table 3; ^{13}C NMR (CD_3OD, 100 MHz) data, see Table 4; HRESIMS *m*/*z* 585.1943 $[M + Na]^+$ (calculated for $C_{28}H_{34}NaO_{12}$, 585.1948).

Table 3. ^1H NMR data of compounds **4**–**6** from *L. robustum* in CD_3OD [a].

No	4b [b]	5 [b]	6 [c]
2	7.43 br. d (7.2)	7.39 br. d (7.2)	7.36 br. d (7.8)
3	7.35 br. t (7.2)	7.30 br. t (7.2)	7.29 br. t (7.8)
4	7.28 br. d (7.2)	7.26 br. d (7.2)	7.25 br. d (7.8)
5	7.35 br. t (7.2)	7.30 br. t (7.2)	7.29 br. t (7.8)
6	7.43 br. d (7.2)	7.39 br. d (7.2)	7.36 br. d (7.8)
7	4.68 d (11.6)	4.65 d (12.0)	4.59 d (12.0)
	4.96 d (11.6)	4.87 d (12.0)	4.80 d (12.0)
Glc or Man			
1′	4.42 d (8.0)	4.38 d (8.0)	4.33 d (7.8)
2′	3.46 dd (9.2, 8.0)	3.38 m	3.37 m
3′	3.76 t (9.2)	3.52 t (8.8)	3.49 t (9.0)
4′	4.90 m	3.43 m	3.37 m
5′	3.54 m	3.52 m	3.49 m
6′	3.56 m	4.38 dd (12.0, 3.6)	4.30 dd (12.0, 6.0)
	3.64 m	4.52 dd (12.0, 2.0)	4.50 dd (12.0, 1.8)

Table 3. *Cont.*

No	4b [b]	5 [b]	6 [c]
Rha			
1″	5.16 d (1.6)	5.17 d (2.0)	5.15 d (1.8)
2″	3.92 dd (3.2, 1.6)	3.94 dd (3.6, 2.0)	3.93 dd (3.0, 1.8)
3″	3.58 m	3.70 dd (9.6, 3.6)	3.70 dd (9.6, 3.0)
4″	3.29 t (9.6)	3.39 m	3.39 t (9.6)
5″	3.56 m	4.00 dd (9.6, 6.4)	3.99 dd (9.6, 6.0)
6″	1.16 d (6.0)	1.24 d (6.4)	1.24 d (6.0)
Cou			
2‴	7.73 d (8.8)	7.46 d (8.4)	7.66 d (8.4)
3‴	6.76 d (8.8)	6.79 d (8.4)	6.76 d (8.4)
5‴	6.76 d (8.8)	6.79 d (8.4)	6.76 d (8.4)
6‴	7.73 d (8.8)	7.46 d (8.4)	7.66 d (8.4)
7‴	6.95 d (12.8)	7.66 d (16.0)	6.90 d (13.2)
8‴	5.80 d (12.8)	6.38 d (16.0)	5.82 d (13.2)

[a] Coupling constants (*J* values in Hz) are shown in parentheses. [b] At 400 MHz. [c] At 600 MHz.

Table 4. ^{13}C NMR data of compounds **4–6** from *L. robustum* in CD_3OD.

No	4b [a]	5 [b]	6 [a]
1	139.0	138.8	138.8
2	129.3	129.3	129.4
3	129.1	129.2	129.3
4	128.7	128.8	128.8
5	129.1	129.2	129.3
6	129.3	129.3	129.4
7	72.0	72.0	72.0
Glc or Man			
1′	103.2	103.1	103.1
2′	76.2	75.7	75.6
3′	81.6	83.9	84.1
4′	70.6	70.4	70.5
5′	76.1	75.5	75.4
6′	62.4	64.6	64.5
Rha			
1″	103.0	102.7	102.8
2″	72.3	72.3	72.4
3″	72.0	72.2	72.3
4″	73.8	74.0	74.0
5″	70.4	70.0	70.0
6″	18.2	17.9	17.9
Cou			
1‴	127.5	126.7	127.4
2‴	134.2	131.3	133.8
3‴	115.8	117.1	116.1
4‴	160.4	162.2	160.6
5‴	115.8	117.1	116.1
6‴	134.2	131.3	133.8
7‴	147.3	147.0	145.3
8‴	115.8	114.5	116.1
CO	166.9	169.2	168.2

[a] At 100 MHz. [b] At 150 MHz.

Compound **5**: yellowish amorphous powder. $[\alpha]^{20}_{D}$ −18.5 (*c* 0.18, MeOH); UV (MeOH) λ_{max} (log ε): 210 (3.9), 230 (3.9), 315 (4.4) nm; IR (film) ν_{max}: 3369, 2925, 2854, 1706, 1605, 1512, 1452, 1164, 1038, 836, 700 cm^{-1}; ^{1}H NMR (CD_3OD, 400 MHz) data, see Table 3; ^{13}C NMR (CD_3OD, 150 MHz) data, see Table 4; HRESIMS *m*/*z* 585.1947 $[M + Na]^+$ (calculated for $C_{28}H_{34}NaO_{12}$, 585.1948).

Compound **6**: white amorphous powder. $[\alpha]^{20}_{D}$ −18.5 (*c* 0.18, MeOH); UV (MeOH) λ_{max} (log ε): 210 (3.9), 230 (3.9), 316 (4.4) nm; IR (film) ν_{max}: 3369, 2925, 2854, 1706, 1605, 1512, 1452, 1164, 1038, 836, 700 cm^{-1}; ^{1}H NMR (CD_3OD, 600 MHz) data, see Table 3; ^{13}C NMR (CD_3OD, 100 MHz) data, see Table 4; HRESIMS *m*/*z* 585.1949 $[M + Na]^+$ (calculated for $C_{28}H_{34}NaO_{12}$, 585.1948).

2.4. Acid Hydrolysis of Compounds 1–6

Compounds **1**–**6** (2 mg), dissolved in 0.1 mL MeOH, were injected into 2 mL H_2SO_4 aqueous solution (1 M) and hydrolyzed at 95 °C for 6 h, respectively. Then, 2 mL $Ba(OH)_2$ solution (1 M) was added. The hydrolyzed solution was filtered and condensed. The monosaccharides in the condensed solution were affirmed by TLC (EtOAc- MeOH-HOAc-H_2O, 8:1:1:0.7, 2 developments) with authentic samples [13]. The R_f values of D-mannose, D-glucose, and L-rhamnose were 0.46, 0.43, and 0.73, respectively.

2.5. Enzymatic Hydrolysis of Compounds 2

Compound **2** (20 mg) and cellulase (30 mg) were added to 12 mL HOAc-NaOAc buffer solution (pH 5.0) and kept at 37 °C for 6 h. The hydrolyzed product was extracted with EtOAc and purified on a silica gel column (eluting with EtOAc) to afford (*R*)-(-)-l-(3,4-dihydroxyphenyl)ethane-l,2-diol and (*S*)-(+)-l-(3,4-dihydroxyphenyl)ethane- l,2-diol (9:11) confirmed by $[\alpha]^{27}_{D}$ +4.8 (*c* 0.15, EtOAc) [17].

2.6. Determination of Bioactivities

The inhibitory effects on FAS, α-glucosidase and α-amylase, and the DPPH and ABTS radical scavenging activities of compounds **1**–**11** were determined by the reported methods [12,13,18,19], while orlistat, acarbose, and L-(+)-ascorbic acid were applied as the positive controls, respectively (Supplementary Material S1).

2.7. Statistical Analyses

Statistical analyses were performed on GraphPad Prism 5.01. All samples were determined in triplicate. The IC_{50} (the ultimate concentration of sample needed to inhibit 50% of enzyme activity or clear away 50% of free radicals) was acquired by plotting the inhibition or scavenging percentage of every sample against its concentration. The results are recorded as mean ± standard deviation (SD). Differences of means between several groups were analyzed by one-way analysis of variance (ANOVA) on the statistical package SPSS 25.0. The differences between groups were deemed to be significant when $p < 0.05$.

3. Results and Discussion

3.1. Identification of Compounds 1–11

Compound **1** was analyzed as $C_{35}H_{46}O_{17}$ by HRESIMS (*m*/*z* 761.2634 $[M + Na]^+$, calculated 761.2633 for $C_{35}H_{46}NaO_{17}$). The NMR spectra of **1** showed 2 stereoisomers **1a** and **1b** (5:1). The ^{1}H and ^{13}C NMR data of **1a** (Supplementary Material S2.) was in agreement with those of 2-(4-hydroxyphenyl)ethyl 3-*O*-[α-L-rhamnopyranosyl-(1→4)-α-L-rhamnopyranosyl]-6-*O*-(*trans*-*p*-coumaroyl)-*O*-β-D-mannopyranoside (ligurobustoside R) [12]. The NMR data of **1b** (Tables 1 and 2) were similar to those of **1a**, except the *trans*-*p*-coumaroyl [δ_H 7.62, 6.35 (1H each, d, *J* = 16.0 Hz, H-7‴, H-8‴)] in **1a** was replaced by the *cis*-*p*-coumaroyl [δ_H 6.86, 5.79 (1H each, d, *J* = 12.8 Hz, H-7‴, H-8‴)] in **1b**. The acid hydrolysis experiment of **1** gave D-mannose, and L-rhamnose was affirmed by TLC. The HMBC experiment of **1b** (Figure 2) displayed the long-distance correlations: between δ_H 4.28 (H-1′ of mannosyl) and δ_C 72.3 (C-8 of aglycone), between δ_H 5.17 (H-1″ of inner rhamnosyl) and δ_C 83.6 (C-3′ of mannosyl), between δ_H 5.19 (H-1‴ of outer rhamnosyl) and δ_C 81.1 (C-4″ of inner rhamnosyl), and between δ_H 4.29 (H-6′a of mannosyl), 4.46 (H-6′b of mannosyl) and δ_C 168.1 (carbonyl of coumaroyl). The ^{1}H and ^{13}C NMR signals of **1b** were assigned by the HMBC experiment (Figure S1). So **1b** was identified as 2-(4-hydroxyphenyl)ethyl 3-*O*-[α-L-rhamnopyranosyl-(1→4)-α-L-rhamnopyranosyl]-6-*O*-(*cis*-

p-coumaroyl)-*O*-*β*-D-mannopyranoside. It is a novel phenylethanoid glycoside named ligurobustoside R_1. In conclusion, compound **1** is a mixture of ligurobustosides R and R_1.

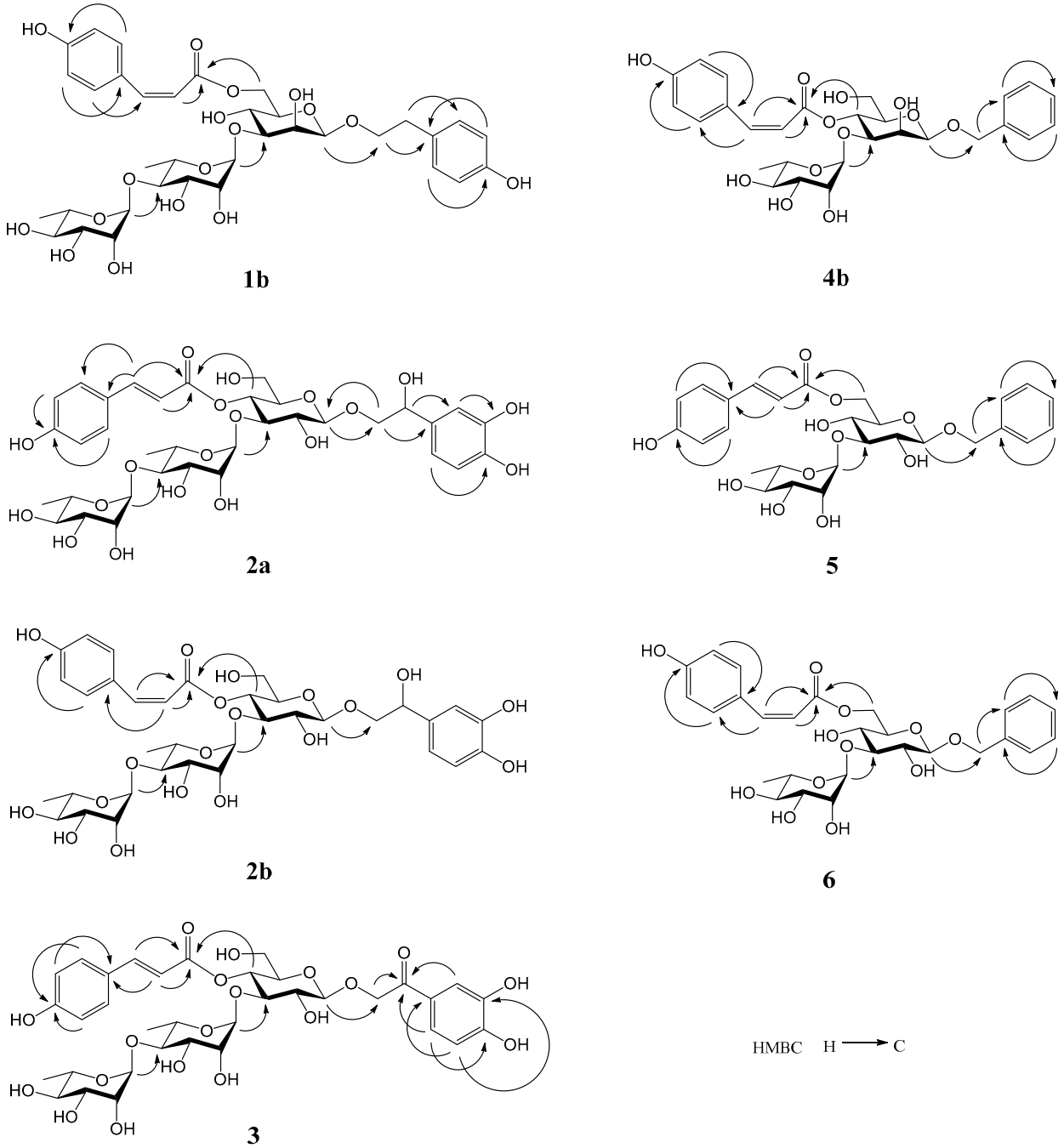

Figure 2. Key HMBC correlations of compounds **1**–**6**.

Compound **2** was analyzed as $C_{35}H_{46}O_{19}$ by HRESIMS (*m*/*z* 793.2536 $[M + Na]^+$, calculated 793.2531 for $C_{35}H_{46}NaO_{19}$). The NMR spectra of **2** showed 2 stereoisomers **2a** and **2b** (10:3). The ^{1}H NMR spectrum of **2a** (Table 1) revealed the following signals: (1) a 4-substituted phenyl at δ_H 6.82, 7.49 (2H each, d, *J* = 8.8 Hz); (2) a 3,4-disubstituted phenyl at δ_H 6.72 (1H, d, *J* = 2.0 Hz), 6.74 (1H, d, *J* = 8.0 Hz), and 6.83 (1H, dd, *J* = 8.0, 2.0 Hz); (3) a trans double bond at δ_H 7.67 and 6.33 (1H each, d, *J* = 16.0 Hz); (4) three anomeric protons at δ_H 4.41 (1H, d, *J* = 8.0 Hz), 5.04 (1H, d, *J* = 2.0 Hz), and 5.22 (1H, d, *J* = 2.0 Hz); (5) a methylene at δ_H 3.56–3.72 (1H, m) and 3.90–3.98 (1H, m), a methyne at δ_H 4.75 (1H, dd, *J* = 9.6, 3.2 Hz), and two methyl groups at δ_H 1.04 (3H, d, *J* = 6.0 Hz) and 1.09 (3H, d, *J* = 6.0 Hz). The

^{13}C NMR spectrum of **2a** (Table 2) showed a carbonyl at δ_C 168.1, 2 phenyl groups at δ_C 114.6–161.5, a double bond at δ_C 114.7 and 147.6, 3 anomeric carbons at δ_C 102.6–104.6, 13 sugar carbons at δ_C 62.2–81.6, a methylene at δ_C 76.7, a methyne at δ_C 74.2, and 2 methyl groups at δ_C 17.7 and 19.1. The above ^{1}H and ^{13}C NMR features of **2a** were related closely to those of (2*R*)-2-hydroxy-2-(3,4-dihydroxyphenyl)ethyl 3-*O*-[*α*-L-rhamnopyranosyl-(1→4)-*α*-L-rhamnopyranosyl]-4-*O*-(*trans*-caffeoyl)-*O*-*β*-D-glucopyranoside (ligurobustoside P) [7], except that the *trans*-caffeoyl in ligurobustoside P was replaced by the *trans*-*p*-coumaroyl in **2a**. The acid hydrolysis experiment of **2** gave D-glucose, and L-rhamnose was affirmed by TLC. Furthermore, the HMBC experiment of **2a** (Figure 2) displayed the long-distance correlations: between δ_H 4.41 (H-1′ of glucosyl) and δ_C 76.7 (C-8 of aglycone), between δ_H 5.22 (H-1″ of inner rhamnosyl) and δ_C 81.2 (C-3′ of glucosyl), between δ_H 5.04 (H-1‴ of outer rhamnosyl) and δ_C 81.6 (C-4″ of inner rhamnosyl), and between δ_H 4.95 (H-4′ of glucosyl) and δ_C 168.1 (carbonyl of coumaroyl). The ^{1}H and ^{13}C NMR signals of **2** were assigned by ^{1}H-^{1}H COSY, HSQC, and HMBC experiments (Figure S2). Thus, the plane structure of **2a** was elucidated as 2-hydroxy-2-(3,4-dihydroxyphenyl)ethyl 3-*O*-[*α*-L-rhamnopyranosyl-(1→4)-*α*-L-rhamnopyranosyl]-4-*O*-(*trans*-*p*-coumaroyl)-*O*-*β*-D-glucopyranoside.

The NMR data of **2b** (Tables 1 and 2) were similar to those of **2a**, except the *trans*-*p*-coumaroyl in **2a** was replaced by the *cis*-*p*-coumaroyl [δ_H 6.99, 5.76 (1H each, d, J = 12.8 Hz, H-7‴″, H-8‴″)] in **2b**. The HMBC experiment of **2b** (Figure 2) displayed the long-distance correlations: between δ_H 4.43 (H-1′ of glucosyl) and δ_C 76.7 (C-8 of aglycone), between δ_H 5.21 (H-1″ of inner rhamnosyl) and δ_C 81.1 (C-3′ of glucosyl), between δ_H 5.06 (H-1‴ of outer rhamnosyl) and δ_C 81.5 (C-4″ of inner rhamnosyl), and between δ_H 4.90 (H-4′ of glucosyl) and δ_C 166.8 (carbonyl of coumaroyl). Therefore, the plane structure of **2b** was identified as 2-hydroxy-2-(3,4-dihydroxyphenyl)ethyl 3-*O*-[*α*-L-rhamnopyranosyl-(1→4)-*α*-L-rhamnopyranosyl]-4-*O*-(*cis*-*p*-coumaroyl)-*O*-*β*-D-glucopyranoside.

In addition, the enzymatic hydrolysis experiment of **2** gave (*R*)-(-)-l-(3,4-dihydroxyphenyl) ethane-l,2-diol and (*S*)-(+)-l-(3,4-dihydroxyphenyl)ethane-l,2-diol (9:11), meaning that *R*/*S* (9:11) was not equal to **2a**/**2b** (10:3). Based on the above evidence, compound **2** was characterized as a mixture of (2*R*/*S*)-2-hydroxy-2-(3,4-dihydroxyphenyl)ethyl 3-*O*-[*α*-L-rhamnopyranosyl-(1→4)-*α*-L-rhamnopyranosyl]-4-*O*-(*trans*-*p*-coumaroyl)-*O*-*β*-D-glucopyranoside and (2*R*/*S*)-2-hydroxy-2-(3,4-dihydroxyphenyl)ethyl 3-*O*-[*α*-L-rhamnopyranosyl-(1→4)-*α*-L-rhamnopyranosyl]-4-*O*-(*cis*-*p*-coumaroyl)-*O*-*β*-D-glucopyranoside. It is a novel phenylethanoid glycoside named ligurobustoside $R_{2–3}$.

Compound **3** was determined as $C_{35}H_{44}O_{19}$ by HRESIMS (m/z 791.2371 $[M + Na]^+$, calculated 791.2374 for $C_{35}H_{44}NaO_{19}$). The ^{1}H NMR spectrum of **3** (Table 1) showed the following signals: (1) a 4-substituted phenyl at δ_H 6.87, 7.54 (2H each, d, J = 8.4 Hz); (2) a 3,4-disubstituted phenyl at δ_H 6.89 (1H, d, J = 8.4 Hz), 7.46 (1H, br. s) and 7.47 (1H, br. d, J = 8.4 Hz); (3) a trans double bond at δ_H 7.68 and 6.37 (1H each, d, J = 16.0 Hz); (4) three anomeric protons at δ_H 4.54 (1H, d, J = 7.6 Hz), 5.06 (1H, br. s) and 5.22 (1H, br. s); (5) a methylene at δ_H 4.98 and 5.26 (1H each, d, J = 16.8 Hz), and two methyl groups at δ_H 1.06 (3H, d, J = 6.0 Hz) and 1.10 (3H, d, J = 6.0 Hz). The ^{13}C NMR spectrum of **3** (Table 2) revealed 2 carbonyl groups at δ_C 167.6 and 196.4, 2 phenyl groups at δ_C 115.8–161.4, a double bond at δ_C 114.9 and 147.3, 3 anomeric carbons at δ_C 102.6–103.9, 13 sugar carbons at δ_C 62.2–81.2, a methylene at δ_C 72.2, and 2 methyl groups at δ_C 18.1 and 19.4. The above ^{1}H and ^{13}C NMR characteristics of **3** were similar to those of **2a**, except that the methyne (C-7 of aglycone) linking with hydroxy in **2a** was replaced by the carbonyl in **3**. The acid hydrolysis experiment of **3** afforded D-glucose and L-rhamnose affirmed by TLC. Additionally, the HMBC experiment of **3** (Figure 2) displayed the long-distance correlations: between δ_H 7.46 (H-2), 7.47 (H-6), 4.98 (H-8a), 5.26 (H-8b) and δ_C 196.4 (C-7), between δ_H 4.54 (H-1′ of glucosyl) and δ_C 72.2 (C-8 of aglycone), between δ_H 5.22 (H-1″ of inner rhamnosyl) and δ_C 81.1 (C-3′ of glucosyl), between δ_H 5.06 (H-1‴ of outer rhamnosyl) and δ_C 81.2 (C-4″ of inner rhamnosyl), and between δ_H 4.96 (H-4′ of glucosyl) and δ_C 167.6 (carbonyl of coumaroyl). The ^{1}H and ^{13}C NMR signals of **3** were assigned by ^{1}H-^{1}H COSY, HSQC, and HMBC experiments (Figure S3). Therefore, compound **3** was determined to be 2-(3,4-

dihydroxyphenyl)-2-oxoethyl 3-*O*-[*α*-L-rhamnopyranosyl-(1→4)-*α*-L-rhamnopyranosyl]-4-*O*-(*trans*-*p*-coumaroyl)-*O*-*β*-D-glucopyranoside. It is a novel phenylethanoid glycoside named ligurobustoside R_4.

Compound **4** was determined as $C_{28}H_{34}O_{12}$ by HRESIMS (*m*/*z* 585.1943 $[M + Na]^+$, calculated 585.1948 for $C_{28}H_{34}NaO_{12}$). The NMR spectra of **4** exhibited 2 stereoisomers **4a** and **4b** (2:1). The ^1H and ^{13}C NMR data of **4a** (Supplementary Material S2.) was in accordance with those of benzyl 3-*O*-(*α*-L-rhamnopyranosyl)-4-*O*-(*trans*-*p*-coumaroyl)-*O*-*β*-D-mannopyranoside (ligurobustoside S) [12]. The NMR data of **4b** (Tables 3 and 4) were very similar to those of **4a**, except the *trans*-*p*-coumaroyl [δ_H 7.67, 6.35 (1H each, d, *J* = 16.0 Hz, H-7‴, H-8‴)] in **4a** was replaced by the *cis*-*p*-coumaroyl [δ_H 6.95, 5.80 (1H each, d, *J* = 12.8 Hz, H-7‴, H-8‴)] in **4b**. The acid hydrolysis experiment of **4** offered D-mannose and L-rhamnose confirmed by TLC. The HMBC experiment of **4b** (Figure 2) displayed the long-distance correlations: between δ_H 4.42 (H-1′ of mannosyl) and δ_C 72.0 (C-7 of aglycone), between δ_H 5.16 (H-1″ of rhamnosyl) and δ_C 81.6 (C-3′ of mannosyl), and between δ_H 4.90 (H-4′ of mannosyl) and δ_C 166.9 (carbonyl of coumaroyl). The ^1H and ^{13}C NMR signals of **4** were assigned by the HMBC experiment (Figure S4). So **4b** was identified as benzyl 3-*O*-(*α*-L-rhamnopyranosyl)-4-*O*-(*cis*-*p*-coumaroyl)-*O*-*β*-D-mannopyranoside. It is a new phenylmethanoid glycoside named ligurobustoside S_1. In sum, compound **4** is a mixture of ligurobustosides S and S_1.

Compound **5** was determined as $C_{28}H_{34}O_{12}$ by HRESIMS (*m*/*z* 585.1947 $[M + Na]^+$, calculated 585.1948 for $C_{28}H_{34}NaO_{12}$). The ^1H NMR spectrum of **5** (Table 3) showed the following signals: (1) a 4-substituted phenyl at δ_H 6.79, 7.46 (2H each, d, *J* = 8.4 Hz); (2) a phenyl at δ_H 7.26 (1H, br. d, *J* = 7.2 Hz), 7.30 (2H, br. t, *J* = 7.2 Hz), and 7.39 (2H, br. d, *J* = 7.2 Hz); (3) a trans double bond at δ_H 7.66 and 6.38 (1H each, d, *J* = 16.0 Hz); (4) two anomeric protons at δ_H 4.38 (1H, d, *J* = 8.0 Hz) and 5.17 (1H, d, *J* = 2.0 Hz); (5) a methylene at δ_H 4.65 and 4.87 (1H each, d, *J* = 12.0 Hz), and a methyl at δ_H 1.24 (3H, d, *J* = 6.4 Hz). The ^{13}C NMR spectrum of **5** (Table 4) revealed a carbonyl at δ_C 169.2, two phenyl groups at δ_C 117.1–162.2, a double bond at δ_C 114.5 and 147.0, two anomeric carbons at δ_C 102.7 and 103.1, nine sugar carbons at δ_C 64.6–83.9, a methylene at δ_C 72.0, and a methyl at δ_C 17.9. The above ^1H and ^{13}C NMR characteristics of **5** were similar to those of benzyl 6-*O*-[(*E*)-3-(3,4-dihydroxyphenyl)-prop-2-enoyl]-3-*O*-(*α*-L-rhamnopyranosyl)-*O*-*β*-D-glucopyranoside (salsaside A) [20], except the *trans*-caffeoyl in salsaside A was replaced by the *trans*-*p*-coumaroyl in **5**. The acid hydrolysis experiment of **5** yielded D-glucose and L-rhamnose identified by TLC. The HMBC experiment of **5** (Figure 2) displayed the long-distance correlations: between δ_H 4.38 (H-1′ of glucosyl) and δ_C 72.0 (C-7 of aglycone), between δ_H 5.17 (H-1″ of rhamnosyl) and δ_C 83.9 (C-3′ of glucosyl), and between δ_H 4.38 (H-6′a of glucosyl), 4.52 (H-6′b of glucosyl) and δ_C 169.2 (carbonyl of coumaroyl). The ^1H and ^{13}C NMR signals of **5** were assigned by ^1H-^1H COSY, HSQC, and HMBC experiments (Figure S5). Therefore, compound **5** was elucidated to be benzyl 3-*O*-(*α*-L-rhamnopyranosyl)-6-*O*-(*trans*-*p*-coumaroyl)-*O*-*β*-D-glucopyranoside. It is a new phenylmethanoid glycoside named ligurobustoside S_2.

Compound **6** was analyzed as $C_{28}H_{34}O_{12}$ by HRESIMS (*m*/*z* 585.1949 $[M + Na]^+$, calculated 585.1948 for $C_{28}H_{34}NaO_{12}$). The ^1H and ^{13}C NMR data of **6** (Tables 3 and 4) were related closely to those of **5**, except the *trans*-*p*-coumaroyl [δ_H 7.66, 6.38 (1H each, d, *J* = 16.0 Hz, H-7‴, H-8‴)] in **5** was replaced by the *cis*-*p*-coumaroyl [δ_H 6.90, 5.82 (1H each, d, *J* = 13.2 Hz, H-7‴, H-8‴)] in **6**. The acid hydrolysis experiment of **6** yielded D-glucose and L-rhamnose affirmed by TLC. The HMBC experiment of **6** (Figure 2) showed the long-distance correlations: between δ_H 4.33 (H-1′ of glucosyl) and δ_C 72.0 (C-7 of aglycone), between δ_H 5.15 (H-1″ of rhamnosyl) and δ_C 84.1 (C-3′ of glucosyl), and between δ_H 4.30 (H-6′a of glucosyl), 4.50 (H-6′b of glucosyl) and δ_C 168.2 (carbonyl of coumaroyl). The ^1H and ^{13}C NMR signals of **6** were assigned by ^1H-^1H COSY, HSQC, and HMBC experiments (Figure S6). Thus, compound **6** was identified as benzyl 3-*O*-(*α*-L-rhamnopyranosyl)-6-*O*-(*cis*-*p*-coumaroyl)-*O*-*β*-D-glucopyranoside. It is a new phenylmethanoid glycoside named ligurobustoside S_3.

Compounds **7–11** (^{1}H, ^{13}C NMR data see S2.) were identified as reported ligupurpuroside B (**7**) [21], *cis*-ligupurpuroside B (**8**) [21,22], ligurobustoside N (**9**) [1], osmanthuside D (**10**) [23], and (*Z*)-osmanthuside B$_6$ (**11**) [23,24], by comparison with published NMR data and 2D-NMR experiments (^{1}H-^{1}H COSY, HSQC, and HMBC). Compounds **8**, **10,** and **11** were isolated from this plant for the first time.

3.2. The Bioactivities of Compounds **1–11**

Compounds **1–11** from the leaves of *L. robustum* were measured for the inhibitory effects on FAS, α-glucosidase, α-amylase, and antioxidant activities. The results of the bioactivity assays are shown in Table 5. As shown in Table 5, the FAS inhibitory effect of compound **11** (IC_{50}: 4.55 ± 0.35 μM) was as strong as the positive control orlistat (IC_{50}: 4.46 ± 0.13 μM), while the FAS inhibitory effects of compounds **4** (IC_{50}: 6.49 ± 0.27 μM) and **9** (IC_{50}: 5.61 ± 0.44 μM) were weaker than orlistat; the α-glucosidase inhibitory effects of compounds **3** and **5** were moderate and weaker than the positive control acarbose; the α-amylase inhibitory effects of compounds **10** and **11** were moderate and weaker than the positive control acarbose; the DPPH radical scavenging activities of compounds **2, 3,** and **9** (IC_{50}: 23.83 ± 0.89~43.17 ± 1.06 μM) were weaker than the positive control L-(+)-ascorbic acid (IC_{50}: 13.66 ± 0.13 μM); the ABTS radical scavenging activities of compounds **3**, **5**, and **7–11** (IC_{50}: 2.68 ± 0.05~4.86 ± 0.06 μM) were stronger than the positive control L-(+)-ascorbic acid (IC_{50}: 10.06 ± 0.19 μM).

Table 5. Results of the bioactivity assays of compounds **1–11** from *L. robustum* [a].

Compounds	FAS IC_{50} (μM) [b]	α-Glucosidase Inhibition at 0.1 mM (%)	α-Amylase Inhibition at 0.1 mM (%)	DPPH IC_{50} (μM) [b]	ABTS•+ IC_{50} (μM) [b]
1	NA [c]	— [d]	—	—	—
2	NA	NA	10.6 ± 2.3 f	43.17 ± 1.06 d	10.62 ± 0.48 f
3	NA	42.3 ± 8.7 bc	NA	23.83 ± 0.89 b	4.13 ± 0.06 c
4	6.49 ± 0.27 c	—	—	—	—
5	NA	45.1 ± 2.5 b	NA	>250	4.86 ± 0.06 d
6	NA	36.5 ± 1.5 c	NA	NA	20.73 ± 0.22 g
7	NA	NA	19.9 ± 1.8 d	>250	2.75 ± 0.09 a
8	NA	NA	NA	>250	4.17 ± 0.06 c
9	5.61 ± 0.44 b	25.4 ± 4.1 d	15.9 ± 3.1 e	29.21 ± 0.37 c	2.68 ± 0.05 a
10	NA	19.3 ± 5.6 e	26.1 ± 1.9 c	>250	3.34 ± 0.02 b
11	4.55 ± 0.35 a	NA	23.5 ± 1.7 c	>250	3.83 ± 0.05 c
Orlistat [e]	4.46 ± 0.13 a				
Acarbose [e]		93.2 ± 0.1 a	51.8 ± 2.5 a		
L-(+)-ascorbic acid [e]				13.66 ± 0.13 a	10.06 ± 0.19 e

[a] Data are recorded as mean ± SD (n = 3). Means with the same letter are not significantly different (one-way analysis of variance, α = 0.05). [b] IC_{50}: the ultimate concentration of sample needed to inhibit 50% of enzyme activity or clear away 50% of free radicals. [c] NA: no activity. [d] It was not measured. [e] Positive control.

The previous study revealed that FAS was a potential therapeutic target for anti-obesity drugs [13,18]; α-glucosidase and α-amylase were two important targets to prevent diabetes and obesity [12,25]; and reactive oxygen species played an important role in the initiation and progression of diabetes [12,26]. Consequently, antioxidants **3–5**, **9**, and **10**, with some FAS, α-glucosidase, and α-amylase inhibitory activities [12], might be a part of the effective ingredients for *L. robustum* to prevent diabetes and obesity.

4. Conclusions

In summary, the phytochemical investigation on the leaves of *L. robustum* resulted in the isolation of eight phenylethanoid glycosides (**1–3**, **7–11**) and three phenylmethanoid glycosides (**4–6**), including six novel compounds (**1b**,**2**,**3**,**4b**,**5**,**6**) identified with spectroscopic method (^{1}H, ^{13}C NMR, ^{1}H-^{1}H COSY, HSQC, HMBC, HRESIMS), and physical and chemical methods. The biological assays showed that the FAS inhibitory effect of compound **11** (IC_{50}: 4.55 ± 0.35 μM) was as strong as the positive control orlistat (IC_{50}: 4.46 ± 0.13 μM); the α-glucosidase inhibitory effects of compounds **3** and **5**, and the α-amylase inhibitory effects of compounds **10** and **11** were moderate; the DPPH radical scavenging activities of

compounds **2**, **3,** and **9** (IC_{50}: 23.83 ± 0.89~43.17 ± 1.06 μM) were weaker than the positive control L-(+)-ascorbic acid (IC_{50}: 13.66 ± 0.13 μM); the ABTS radical scavenging activities of compounds **3**, **5**, and **7**–**11** (IC_{50}: 2.68 ± 0.05~4.86 ± 0.06 μM) were stronger than the positive control L-(+)-ascorbic acid (IC_{50}: 10.06 ± 0.19 μM). Together this work and previous studies [12,13], phenylethanoid, phenylmethanoid, and monoterpenoid glycosides were believed as the main anti-obesity and anti-diabetes components of *L. robustum*. This research offered a theoretical basis for the leaves of *L. robustum* as a functional tea to prevent obesity and diabetes.

Supplementary Materials: The following supporting information can be downloaded at: https://www.mdpi.com/article/10.3390/molecules27217390/s1, ^{1}H NMR, ^{13}C NMR, HMBC, HRESIMS, and IR spectra of compounds **1** (Figure S1) and **4** (Figure S4); ^{1}H NMR, ^{13}C NMR, ^{1}H-^{1}H COSY, HSQC, HMBC, HRESIMS and IR spectra of compounds **2** (Figure S2), **3** (Figure S3), **5** (Figure S5), and **6** (Figure S6); determination of bioactivities (S1.); ^{1}H NMR and ^{13}C NMR data of **1a**, **4a**, and **7**–**11** (S2.).

Author Contributions: Conceptualization, S.-H.L., J.H. and H.-J.Z.; methodology, S.-H.L.; formal analysis, S.-H.L. and R.C.; investigation, S.-H.L., H.-J.Z., R.C., J.-P.P. and X.-X.L.; data curation, J.H.; writing—original draft preparation, S.-H.L.; writing review and editing, J.H. and X.-X.L.; supervision, J.H.; funding acquisition, S.-H.L. All authors have read and agreed to the published version of the manuscript.

Funding: This study was funded by the Guangxi Natural Science Foundation Project (grant number 2020GXNSFAA297129), Guangxi Science and Technology Base and Talents Special Project (grant number Guike AD21075006), and Youjiang Medical University for Nationalities Science Research Project (grant number yy2021sk004).

Institutional Review Board Statement: Not applicable.

Informed Consent Statement: Not applicable.

Data Availability Statement: The data presented in this study are available in Supplementary materials.

Acknowledgments: The authors are grateful to Fu Su and You Zhou, West China School of Pharmacy, Sichuan University, for the NMR measurements. The authors sincerely thank Ming-Hai Tang, State Key Laboratory of Biotherapy, West China Hospital, Sichuan University, for the HRESIMS measurement.

Conflicts of Interest: The authors declare no conflict of interest. The funders had no role in the design of the study; in the collection, analyses, or interpretation of data; in the writing of the manuscript, or in the decision to publish the results.

Sample Availability: Samples of the compounds are not available from the authors.

References

1. He, Z.D.; Lau, K.M.; But, P.P.-H.; Jiang, R.W.; Dong, H.; Ma, S.C.; Fung, K.P.; Ye, W.C.; Sun, H.D. Antioxidative glycosides from the leaves of *Ligustrum robustum*. *J. Nat. Prod.* **2003**, *66*, 851–854. [CrossRef] [PubMed]
2. Yang, R.M.; Liu, F.; He, Z.D.; Ji, M.; Chu, X.X.; Kang, Z.Y.; Cai, D.Y.; Gao, N.N. Anti-obesity effect of total phenylpropanoid glycosides from *Ligustrum robustum* Blume in fatty diet-fed mice via up-regulating leptin. *J. Ethnopharmacol.* **2015**, *169*, 459–465. [CrossRef] [PubMed]
3. Zhu, F.; Cai, Y.Z.; Sun, M.; Ke, J.X.; Lu, D.Y.; Corke, H. Comparison of major phenolic constituents and in vitro antioxidant activity of diverse kudingcha genotypes from *Ilex kudingcha, Ilex cornuta*, and *Ligustrum robustum*. *J. Agric. Food Chem.* **2009**, *57*, 6082–6089. [CrossRef]
4. Lau, K.M.; He, Z.D.; Dong, H.; Fung, K.P.; But, P.P.-H. Anti-oxidative, anti-inflammatory and hepato-protective effects of *Ligustrum robustum*. *J. Ethnopharmacol.* **2002**, *83*, 63–71. [CrossRef]
5. Xie, Z.M.; Zhou, T.; Liao, H.Y.; Ye, Q.; Liu, S.; Qi, L.; Huang, J.; Zuo, H.J.; Pei, X.F. Effects of *Ligustrum robustum* on gut microbes and obesity in rats. *World J. Gastroenterol.* **2015**, *21*, 13042–13054. [CrossRef] [PubMed]
6. Li, L.; Peng, Y.; Xu, L.J.; Wu-Lan, T.N.; Shi, R.B.; Xiao, P.G. Chemical constituents from *Ligustrum robustum* Bl. *Biochem. Syst. Ecol.* **2010**, *38*, 398–401. [CrossRef]
7. Li, L.; Peng, Y.; Liu, Y.; Xu, L.J.; Guo, N.; Shi, R.B.; Xiao, P.G. Two new phenethanol glycosides from *Ligustrum robustum*. *Chinese Chem. Lett.* **2011**, *22*, 326–329. [CrossRef]

8. Tian, J.; Zhang, H.J.; Sun, H.D.; Pan, L.T.; Yao, P.; Chen, D.Y. Monoterpenoid glycosides from *Ligustrum robustum*. *Phytochemistry* **1998**, *48*, 1013–1018. [CrossRef]
9. Tian, J.; Sun, H.D. New monoterpenoid glycosides from *Ligustrum robustum*. *Chin. J. Appl. Envir. Biol.* **1999**, *5*, 501–506.
10. Yu, Z.L.; Zeng, W.C. Antioxidant, antibrowning, and cytoprotective activities of *Ligustrum robustum* (Roxb.) Blume extract. *J. Food Sci.* **2013**, *78*, 1354–1362. [CrossRef]
11. Yu, Z.L.; Gao, H.X.; Zhang, Z.; He, Z.; He, Q.; Jia, L.R.; Zeng, W.C. Inhibitory effects of *Ligustrum robustum* (Roxb.) Blume extract on α-amylase and α-glucosidase. *J. Funct. Foods* **2015**, *19*, 204–213. [CrossRef]
12. Lu, S.-H.; Zuo, H.-J.; Shi, J.-X.; Li, C.-R.; Li, Y.-H.; Wang, X.; Li, L.-R.; Huang, J. Two new glycosides from the leaves of *Ligustrum robustum* and their antioxidant activities and inhibitory effects on α-glucosidase and α-amylase. *S. Afr. J. Bot.* **2019**, *125*, 521–526. [CrossRef]
13. Lu, S.-H.; Huang, J.; Zuo, H.-J.; Zhou, Z.-B.; Yang, C.-Y.; Huang, Z.-L. Monoterpenoid glycosides from the leaves of *Ligustrum robustum* and their bioactivities. *Molecules* **2022**, *27*, 3709. [CrossRef] [PubMed]
14. Ito, H.; Otsuki, A.; Mori, H.; Li, P.; Kinoshita, M.; Kawakami, Y.; Tsuji, H.; Fang, D.Z.; Takahashi, Y. Two new monoterpene glycosides from Qing Shan Lu Shui tea with inhibitory effects on leukocyte-type 12-lipoxygenase activity. *Molecules* **2013**, *18*, 4257–4266. [CrossRef]
15. Kawakami, Y.; Otsuki, A.; Mori, Y.; Kanzaki, K.; Suzuki-Yamamoto, T.; Fang, D.Z.; Ito, H.; Takahashi, Y. Involvement of the hydroperoxy group in the irreversible inhibition of leukocyte-type 12-lipoxygenase by monoterpene glycosides contained in the Qing Shan Lu Shui tea. *Molecules* **2019**, *24*, 304. [CrossRef]
16. Wu, Y.; Yang, J.; Liu, X.J.; Zhang, Y.; Lei, A.L.; Yi, R.K.; Tan, F.; Zhao, X. Preventive effect of small-leaved Kuding tea (*Ligustrum robustum*) on high-diet-induced obesity in C57BL/6J mice. *Food Sci. Nutr.* **2020**, *8*, 4512–4522. [CrossRef]
17. Fisher, A.J.; Kerrigan, F. A new convenient synthesis of 1-(3-hydroxy-4-methoxyphenyl)ethane-1,2-diol (iso-MHPG) and its enantiomers. *Synth. Commun.* **1998**, *28*, 2959–2968. [CrossRef]
18. Fan, H.J.; Wu, D.; Tian, W.X.; Ma, X.F. Inhibitory effects of tannic acid on fatty acid synthase and 3T3-L1 preadipocyte. *Biochim. Biophys. Acta* **2013**, *1831*, 1260–1266. [CrossRef]
19. Wu, D.; Ma, X.F.; Tian, W.X. Pomegranate husk extract, punicalagin and ellagic acid inhibit fatty acid synthase and adipogenesis of 3T3-L1 adipocyte. *J. Func. Foods* **2013**, *5*, 633–641. [CrossRef]
20. Lei, L.; Jiang, Y.; Liu, X.M.; Tu, P.F.; Wu, L.J.; Chen, F.K. New glycosides from *Cistanche salsa*. *Helv. Chim. Acta* **2007**, *90*, 79–85. [CrossRef]
21. He, Z.D.; Liu, Y.Q.; Yang, C.R. Glycosides from *Ligustrum purpurascens*. *Acta Bot. Yunnanica* **1992**, *14*, 328–336.
22. Fan Wong, I.Y.; He, Z.-D.; Huang, Y.; Chen, Z.-Y. Antioxidative activities of phenylethanoid glycosides from *Ligustrum purpurascens*. *J. Agric. Food Chem.* **2001**, *49*, 3113–3119. [CrossRef] [PubMed]
23. Sugiyama, M.; Kikuchi, M. Studies on the constituents of *Osmanthus* species. VI. Structures of phenylpropanoid glycosides from the leaves of *Osmanthus asiaticus* Nakai. *Chem. Pharm. Bull.* **1990**, *38*, 2953–2955. [CrossRef]
24. Zhang, J.Y.; Li, C.; Che, Y.Y.; Wu, J.R.; Wang, Z.J.; Cai, W.; Li, Y.; Ma, Z.G.; Tu, P.F. LTQ-Orbitrap-based strategy for traditional Chinese medicine targeted class discovery, identification and herbomics research: A case study on phenylethanoid glycosides in three different species of Herba Cistanches. *RSC Adv.* **2015**, *5*, 80816–80828. [CrossRef]
25. Mudgil, P.; Kamal, H.; Yuen, G.C.; Maqsood, S. Characterization and identification of novel antidiabetic and anti-obesity peptides from camel milk protein hydrolysates. *Food Chem.* **2018**, *259*, 46–54. [CrossRef] [PubMed]
26. Zhao, J.Q.; Wang, Y.M.; Yang, Y.L.; Zeng, Y.; Wang, Q.L.; Shao, Y.; Mei, L.J.; Shi, Y.P.; Tao, Y.D. Isolation and identification of antioxidant and α-glucosidase inhibitory compounds from fruit juice of *Nitraria tangutorum*. *Food Chem.* **2017**, *227*, 93–101. [CrossRef]